

Phased-array antennas using novel PSoC-controlled phase shifters for wireless applications

Aparna B. Barbadekar^{1,2}  and Pradeep M. Patil³

¹Department of Electronics and Telecommunication Engineering, AISSMS IOIT, Pune, India; ²Department of Electronics and Telecommunication Engineering, VIIT, Pune, India and ³SNDCOERC, Yeola, Dist. Nashik, India

Research Paper

Cite this article: Barbadekar AB, Patil PM (2022). Phased-array antennas using novel PSoC-controlled phase shifters for wireless applications. *International Journal of Microwave and Wireless Technologies* **14**, 879–891. <https://doi.org/10.1017/S1759078721001094>

Received: 8 March 2021

Revised: 18 June 2021

Accepted: 20 June 2021

First published online: 21 July 2021

Key words:

Dipole antenna; ISM band; phase shifter; power divider; PSoC

Author for correspondence:

Aparna B. Barbadekar,

E-mail: barbadekar.aparna@gmail.com

Abstract

The paper proposes a system consisting of novel programmable system on chip (PSoC)-controlled phase shifters which in turn guides the beam of an antenna array attached to it. Four antennae forming an array receive individual inputs from the programmable phase shifters (IC 2484). The input to the PSoC-based phase shifter is provided from an optimized 1:4 Wilkinson power divider. The antenna consists of an inverted L-shaped dipole on the front and two mirrored inverted L-shaped dipoles mounted on a rectangular conductive structure on the back which resonates in the ISM/Wi-Fi band (2.40–2.48 GHz). The power divider is designed to provide the feed to the phase shifter using a beamforming network while ensuring good isolation among the ports. The power divider has measured S_{11} , S_{21} , S_{31} , S_{41} , and S_{51} to be -14 , -6.25 , -6.31 , -6.28 , and -6.31 dB, respectively at a frequency of 2.45 GHz. The ingenious controller is designed in-house using a PSoC microcontroller to regulate the control voltage of individual phase shifter IC and generate progressive phase shifts. To validate the calibration of the in-house designed control circuit, the phased array is simulated using s_p^2 touchstone file of IC 2484. This designed control circuit exhibits low insertion loss close to -8.5 dB, voltage standing wave ratio of 1.58:1, and reflection coefficient (S_{11}) is -14.36 dB at 2.45 GHz. Low insertion loss variations confirm that the phased-array antenna gives equal amplitude and phase. The beamforming radiation patterns for different scan angles (30, 60, and 90°) for experimental and simulated phased-array antenna are matched accurately showing the accuracy of the control circuit designed. The average experimental and simulated gain is 13.03 and 13.48 dBi respectively. The in-house designed controller overcomes the primary limitations associated with the present electromechanical phased array such as cost weight, size, power consumption, and complexity in design which limits the use of a phased array to military applications only. The current study with novel design and enhanced performance makes the system worthy of the practical use of phased-array antennas for common society at large.

Introduction

In recent years, the ever-increasing requirements in signal detection and information transmission need fast scanning antennas which are fulfilled successfully by the use of directive antennas in the form of phased antenna arrays [1]. Due to ease of integration, low weight, and lower fabricating costs, the antennas based on the planar substrate have been used in various phased-array structures [2, 3]. More power divider working at millimeter-wave for side-lobe level (SLL) reduction is proposed in [4] where two 1:6 unequally feed power dividers are used. In [5], a combination of power divider and phase shifter is proposed using lumped inductance and capacitance where the concept of composite right-/left-handed transmission line (CRLH-TL) phase characteristic is used. The designed system has a phase shift of 90°. Performance enhancement of parameters such as SLLs, directivity, and beam width are carried out by using two different techniques. The proposed array achieves beam steering using directional hybrid coupler and switched line phase [6]. The important consideration in the form of phase shifting is provided through careful selection of phase delay networks which ultimately depends on the system architecture [7–9]. A phase shifter is interfaced with each antenna to modify the phase association between the signals of antenna elements. Fixed phase shift in the design leads to the passive device while tunable phase shift yields an active antenna. The electronic or mechanical arrangement helps in tuning the phase shift for the phase shifters [10–12].

Shifters are proposed for the improvement of performance parameters. Due to technological developments, there is a remarkable change in the design process of phase shifters. The phased-array deployment faces primary hindrance due to the associated high cost in integrating them with the transmit/receive (T/R) modules. Phase shifters play a critical role

in the T/R modules for creating required phase shifts between the elements of the antenna and also help in steering the beam of the antenna in the desired direction. Mostly, phase shifters lead to half the entire system's cost while implementing phased arrays which are electronically scanned. Various phase shifters using ferrite materials [13], microelectromechanical system structures [14], and solid-state devices [15] are implemented by the researchers. The cost of phased arrays is still too high using these materials and the need for low-cost phase shifters that can be used for phased arrays in low-end profitable products is very much foreseeable in the future. Therefore, there is an immense need for developing the ultra-low-cost next-generation phased arrays using novel tactics.

Researchers have proposed systems [16–18] that steer the beam without using any phase shifters. A cost-effective phased-array patch antenna using the steering of the beam in the absence of phase shifters is proposed in [16]. This novel technique can greatly reduce the cost of a phased-array system and will enable the wide-scale deployment of phased arrays in low-end commercial products. The required phase shifts among the antenna elements are attained by varying the capacitor reactance and are capable of steering the beam between -20 and 20° . The problem with this design is the narrow beam steering range. A novel phase-adjustable and high-power array element is proposed in [17] using a polarization turn reflector. By rotation of driven dipole polarization, the element is capable of providing linear and continuous phases in the far-field region. With the property of phase adjustment, the element is a good substitute for its use as a digital phase shifter. The array achieves beam control with high accuracy in the absence of phase shifters. This design also has the disadvantage of small scanning angles. A linear scanning antenna using two wide angles is presented in [18]. Electric walls combined with a U-shaped wide beamwidth microstrip antenna are used to enhance the scanning performance. A wide-beam antenna with a combination of parasitic patches creatively arranged metallic vias on both the electric dipole sides that helps in enhancing the 3-dB beam-width [19]. The techniques explained here are advantageous however precise and broad beam steering is difficult to achieve. Therefore, the phase shifters that help in solving the problem are in great demand.

Phase shifters integrated with substrate-integrated waveguide (SIW)-based phased-array antennas are proposed in [20, 21]. In [20], a miniaturized C-band phased-array antenna based on a novel series-fed network, radiating elements, and phase shifters is presented. A compact and cost-effective phase shifter using 4-bit CRLH is used considering the easy placement in a series-fed network. A 38° beam scanning range is achieved by the system. A continuously tunable 1×4 phased array SIW phase shifter is presented in [21]. The wide phase disparity is achieved with the help of a phase shifter that is controlled electronically and is constructed by the amalgamation of varactor diodes within a reflection-type construction. The system achieves a beam scanning range from -45 to 45° . In [22], a compact defected reconfigurable microstrip structure-based phase shifter is proposed for its use in phased-array antennas. A complete phase shifter design scheme is described which serves as engineering guidance. A phase shifter with three-step design schemes is presented that switches its beam in the H plane between -15 , 0 , and 15° . An electrical beam steering two-dimensional antenna using a barium-strontium-titanate (BST) thick film is proposed. Sixteen phased-array antennas are controlled using individual phase shifters integrated with a 1:16 feeding network. Phase shifters are

realized using CRLH-TL. The varactor in the form of an interdigital capacitor is used for phase shifters which are integrated with BST thick films printed using inkjet printing. The phase shifter is controlled using a simple biasing and helps in achieving the beam scanning range of $\pm 25^\circ$ along the E and H planes [23]. Monolithic microwave integrated circuit (MMIC) phase shifters such as switch types, reflection type, and vector sum methods were reported in [24] where a 12 GHz, 6-bit switched type phase shifter MMIC is proposed. But, at low microwave frequencies, the value of the capacitors and inductors, and the size of TLs were considerably large and hence the design of phase shifters on chips was difficult. For X-band phased arrays, a 6-bit vector-based control circuit is designed in [25]. A simple technique for generating the phase shift can be very advantageous to avoid designing phase shift networks.

This paper explores the feasibility of the integration of the proposed system with the programmable system on chip (PSoC) approach. PSoC is an entirely new embedded design platform that incorporates the best analog, digital, and microcontroller worlds. Taking into account the unique advantages of the PSoC such as expandability, innovativeness, and reconfigurability, this technology is utilized for the calibration of an analog phase shifter. Here both, the RF components and PSoC are embedded to set control voltages for each phase shifter to generate the directive beam pattern. The phased array using s_p^2 touchstone file of IC 2484 in CST software is also simulated to validate the calibration of the phase shifter. The touchstone files (ASCII proprietary file) incorporate S-parameters specified by frequency-dependent linear network specification.

The contribution of the proposed PSoC-based phase shifter can be summarized as follows:

- (1) Reduces hardware requirement as PSoC is digitally configurable.
- (2) In PSOC, the power requirement of each component/on-chip peripheral can be easily managed. If any peripheral is not required then power to that peripheral can be easily cut-off with the help of supporting software.
- (3) Does not require multiple design revisions as at the design level, each component is managed through software. This makes it easy to redesign the system if any fault or debugging error is detected. Therefore, there is no need for multiple design revisions. This helps in reducing complete system design time and efforts.

The organization of the paper is as follows: Section "Design methodology" describes the design methodology and working principle of the phased-array antenna interfaced with a phase shifter, power divider, and antenna. The PSoC Creator IDE is presented in Section "Proposed system design using PSoC" followed by the simulated system using CST and its validation through the entire assembly setup and measurement of a prototype in Section "Simulated and measured phased-array antenna." Finally, a comparison with the existing literature and conclusions are outlined in Sections "Performance comparison of proposed design" and "Conclusion," respectively.

Design methodology

To better understand the design structure, the circuit configuration of the proposed system using a WPD, PSoC, IC 2484, and antenna array is shown in Fig. 1.

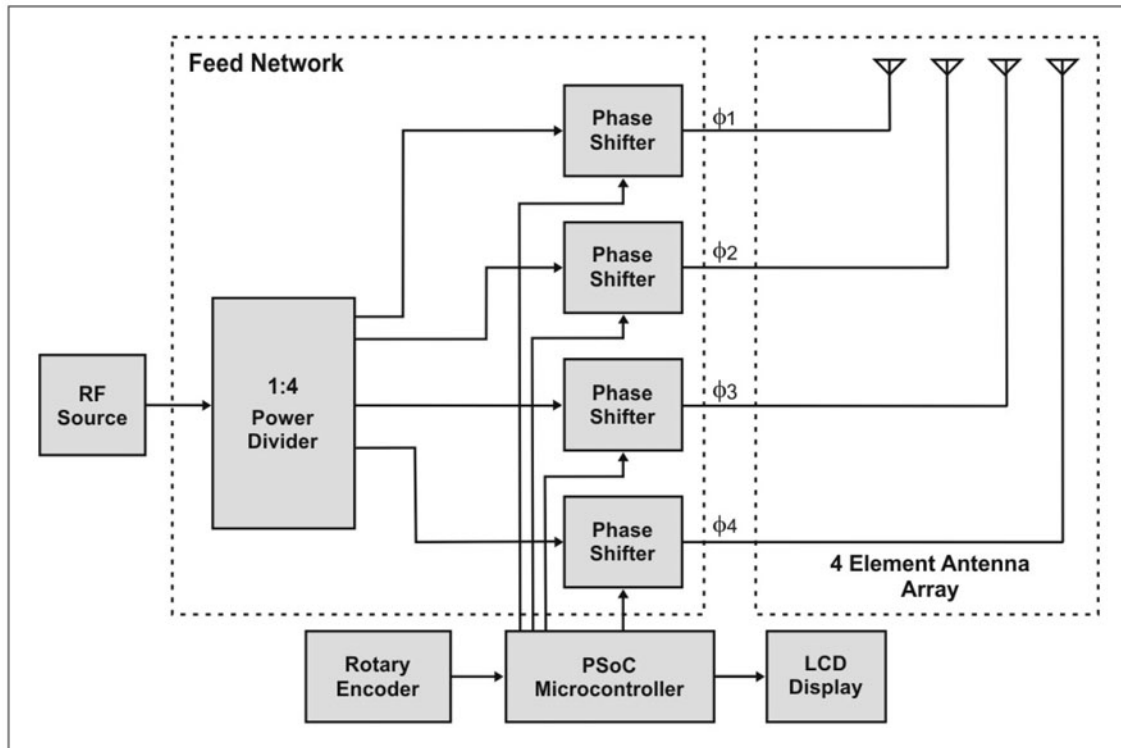


Fig. 1. Design configuration of the proposed system to generate progressive phase shifts.

Power divider design and working principle

Power divider which forms the first block of the overall structure plays an important role in directing the beam to the phase shifters connected across its output ports. Feeding network to the final array antennas is carried out by amalgamation of power divider and phase shift network. The corporate and series feed techniques are used for feeding the antenna arrays where single/multiple TLs are used for feeding the series/corporate network. Fabrication of series feed network is easier however high voltage standing wave ratio (VSWR) due to additive mismatch and progressive phase delay makes it unsuitable for such application. Corporate feed network on the other side offers great flexibility and better control of phase for each array. Individual excitation to array elements with equal power divider and line lengths is supplied by corporate feed.

Figure 2 shows the proposed 1:4 WPD which plays a significant role in communication systems because of its characteristics namely, simple configuration, matching of impedance, and isolation at output ports. The structure of the WPD, as shown in Fig. 2, comprises two $\lambda/4$ TLs at a resonating frequency of 2.45 GHz and the branch impedances $\sqrt{2Z_0}$ and $2Z_0$. The circuit is analyzed using an even-odd mode analysis [22, 23]. The 100 Ω resistors used at the output ports enable the output to match at the same time also ensure better isolation. The fabricated power divider is depicted in Fig. 3 which is printed on the FR-4 substrate (ϵ_r : 4.3, thickness: 1.6 mm) having an overall dimension of 157×112 mm². The WPD acts as a network of corporate feed for feeding the phase shifter with equal phase and amplitude. The output ports have no reflection and hence, they are perfectly isolated.

To comprehend the working principle, the surface current distribution of power divider at 2.45 GHz is shown in Fig. 4 where it can be observed that no coupling current is present between ports

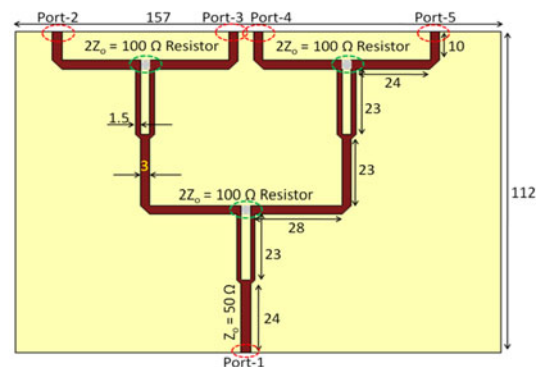


Fig. 2. Schematic geometry of 1:4 Wilkinson power divider (WPD).

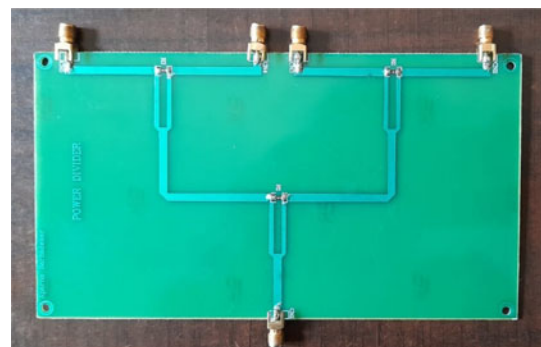


Fig. 3. Fabricated prototype of 1:4 WPD.

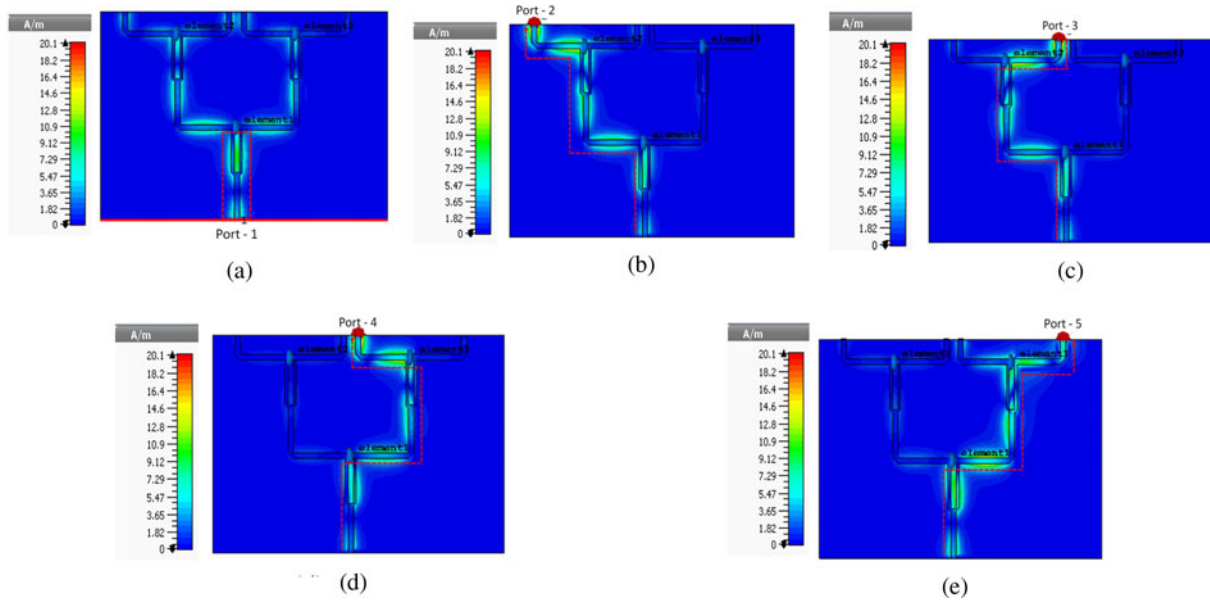


Fig. 4. Surface current at (a) port 1, (b) port 2, (c) port 3, (d) port 4, and (e) port 5.

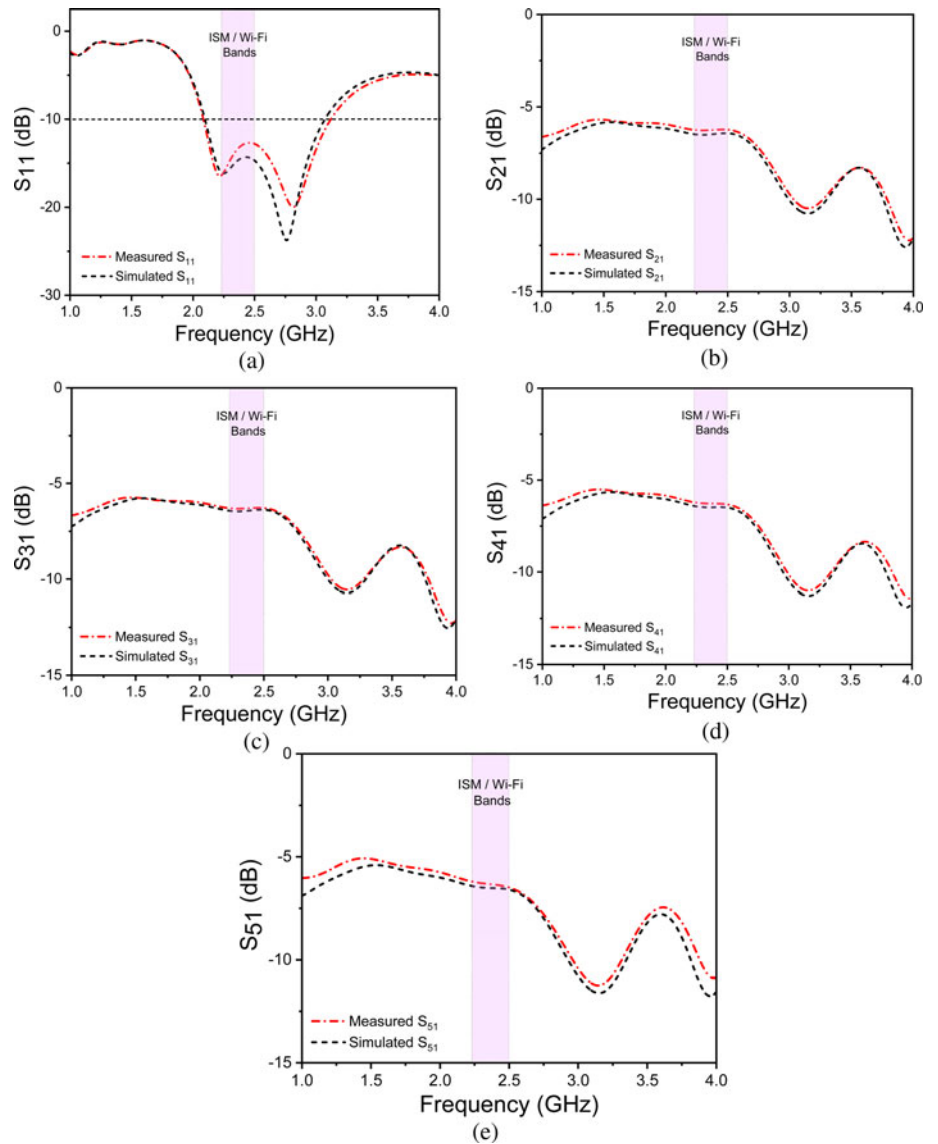


Fig. 5. S-Parameters result of the WPD: (a) S_{11} , (b) S_{21} , (c) S_{31} , (d) S_{41} , and (e) S_{51} .

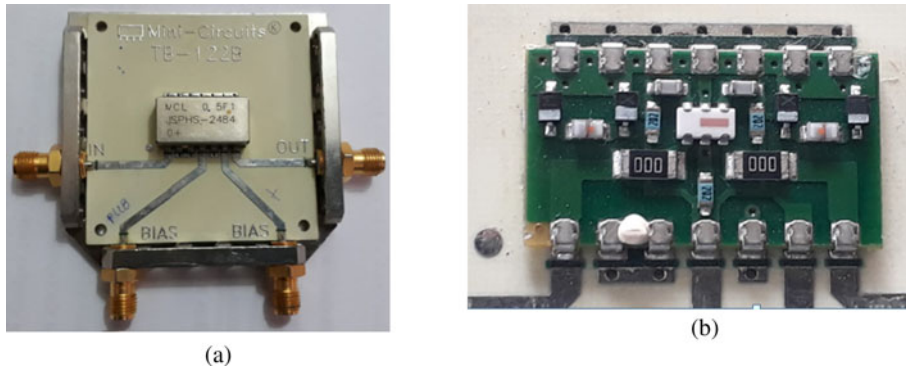


Fig. 6. Phase shifter: (a) top view and (b) inner view.

when port 1 is excited by terminating the other ports and observing the current at the testing port (shown with dotted red line). Further to validate the current distribution when port 2, 3, 4, and 5 are excited, it is observed that the current flows through the designated path only (shown with red-dotted line) in Figs 4(b)–4(e), respectively.

Figure 5 illustrates that the power divider has a measured fractional bandwidth of 39.69%. It can also be visualized that the measured S_{21} , S_{31} , S_{41} , and S_{51} are -6.25 , -6.31 , -6.28 , and -6.31 dB, respectively, which are very low and shows good agreement with the simulated values. It can also be seen that, S_{21} , resembles S_{31} , S_{41} , and S_{51} which indicates that the power has been distributed equally to all the output ports.

From the above analysis, it can be verified that the designed 1:4 power divider shows good performance as it has low insertion loss and good VSWR.

Phase shifter design and working principle

The phase shifter is implemented using an analog variable control voltage IC 2484. The chip is mounted on TB-122B authorized layout printed circuit board (PCB) with internal view as shown in Fig. 6. It is built on a test panel that utilizes grounded co-planar waveguides for input–output RF excitation. The substrate used in the test board PCB is Rogger-R0 4350 with a dielectric constant of 3.5 and a thickness of 0.762 mm. All traces on the test board are made with electrolysis nickel using 1 oz of copper. In order to allow measurements, female sub-miniature version (SMA) connectors are used at both the input and output RF ports.

The four-phase shifter ICs as shown in Fig. 7A are connected in the system layout such that the RF input given to 1:4 WPD equally divides the amplitude and phase and provides the same input to each of the phase shifters. The control voltage from the power supply 0–15 V is regulated through a control switch and is applied to each control pin 6 of the IC 2484. The control voltage is varied in the step of 0.5 V and a set of readings for each individual phase shifter are taken and stored in the look-up table.

The graphs plotted in Figs 7B(a)–7B(d) show the variation of the control voltage versus progressive phase shift. It can be observed from IC 2484 datasheet that the individual phase shifter always shows a positive phase angle when the voltage is varied from 0 to 15 V. However, when phase shifters are used as a feed network, they are supposed to give a progressive phase shift to form a beam in the phased-array antenna. The plotted data confirm that the phase shifters yield both positive and negative phase angles leading to generate progressive phase shift when connected in the system. The phase shift data are stored in the look-up table for further processing with the PSoC controller.

According to the datasheet of IC 2484, VSWR varies from 1.5 to 2 and the reflection coefficient (S_{11}) less than -10 dB is expected. The S_{11} (dB) and VSWR value below -10 dB and 1.58, respectively, are achieved for the band of interest as shown in Figs 8(a) and 8(b), respectively.

To verify the impact of interfacing WPD with phase shifter, the insertion loss is shown in Figs 9(a)–9(d) from ports 2 to 5. It is visualized that the insertion loss from ports 2 to 5 is -8.21 , -8.32 , -8.29 , and -8.39 dB, respectively. These variations may be due to a fabricated power divider and soldering of SMA connectors. After deducting the insertion loss due to the power divider, the net insertion losses that occur due to the phase shifter at ports 2, 3, 4, and 5 are -1.73 , -1.88 , -1.78 , and -1.84 dB, respectively. The average value of the insertion loss is -1.80 dB, which is well within the specified value of 5.6 dB [26].

Antenna design and working principle

Figure 10 illustrates the schematic geometry of antenna having dimensions of 90×96 mm². The antenna consists of an inverted L-shaped dipole on the front as shown in Fig. 10(a) and two mirrored inverted L-shaped dipoles mounted on a rectangular conductive structure on the back as depicted in Fig. 10(b). Via is inserted on the left inverted L-shaped dipole on the back which helps in enhancing the bandwidth. Vias are also incorporated near the feed which helps in getting directive patterns and leads to lowering of back radiation as suggested in [27].

The antenna ground plane evolution in terms of S_{11} from steps 1 to 5 (proposed antenna) design is depicted in Fig. 11. It is observed that by inserting the mirrored inverted L-shaped conductive structures with thick bottom interfaced over a truncated rectangular block from both sides and inserting via helps in substantial bandwidth enhancement spanning from 2.09 to 3.10 GHz.

An FR4 substrate ($\tan \delta = 0.02$, $\epsilon_r = 4.4$) having a thickness of 1.6 mm is used for realizing the dipole antenna. The design parameters of dipole antenna are indicated in Fig. 10 which is achieved after optimizing the antenna dimensions and carrying out the performance analysis in terms of reflection coefficient. The fabricated dipole antenna is illustrated in Figs 12(a) and 12(b).

In order to validate the simulation results, a vector network analyzer Rohde & Schwarz (9 kHz to 13.6 GHz) is used to measure reflection coefficient S_{11} (dB) characteristics and VSWR, while gain and radiation patterns are measured using an anechoic chamber.

Figure 13 shows that the simulated and measured S_{11} curves are matching well with each other. A minimal deviation is found, which may be due to cable losses while used at the

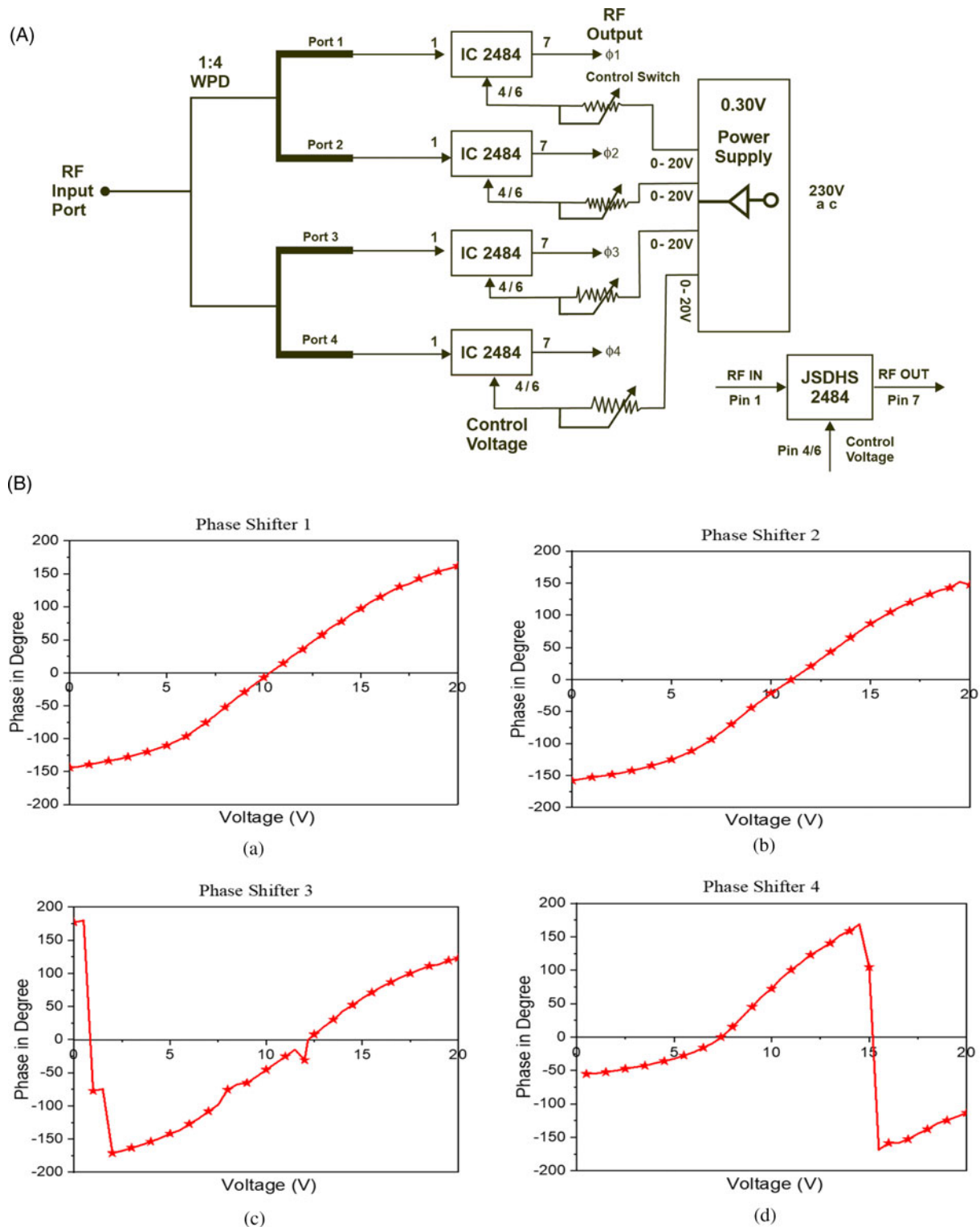


Fig. 7. (A) Block diagram for calibration a phase angle versus control voltage. (B) Variation of phase shift with voltage of (a) phase shifter 1, (b) phase shifter 2, (c) phase shifter 3, and (d) phase shifter 4.

time of measurement, and fabrication tolerances. From Fig. 13, it is visualized that the proposed dipole antenna design exhibits the measured fractional impedance bandwidth of 39.69% (2.08–3.11 GHz) to function smoothly in ISM/Wi-Fi frequency bands.

To verify the range of broadcasting station, nulls, azimuth, and attenuation, the radiation patterns of the proposed dipole antenna in the E -plane (YZ), $\phi = 0^\circ$ and H -plane (XZ), $\phi = 90^\circ$ at 2.45 GHz are depicted in Fig. 14. It is apparent that in the E -plane, main lobe magnitude of 5.52 dB is achieved in the 90° direction

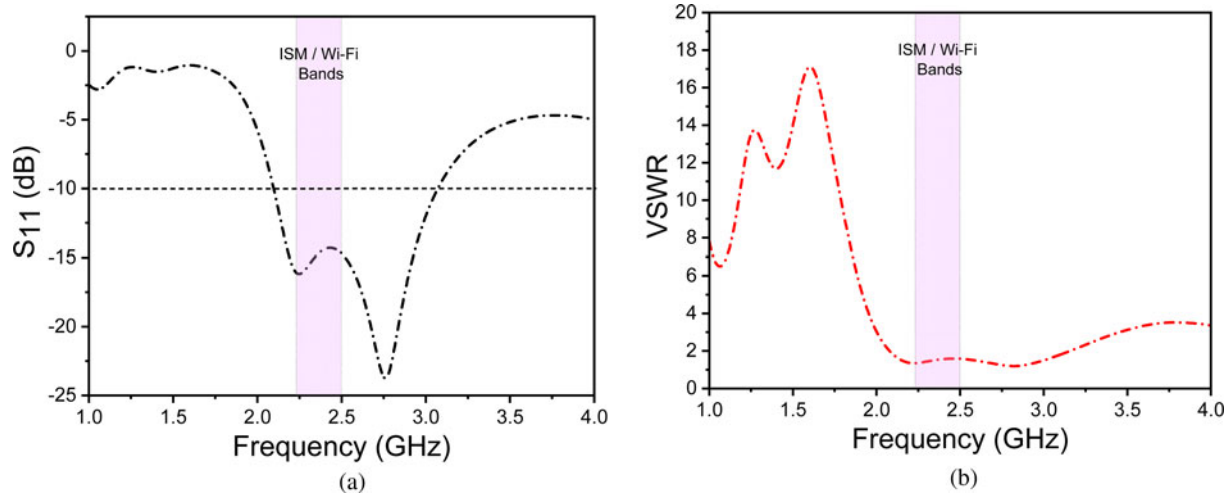


Fig. 8. Frequency versus S_{11} and VSWR of phase shifter: (a) S_{11} (dB) and (b) VSWR.

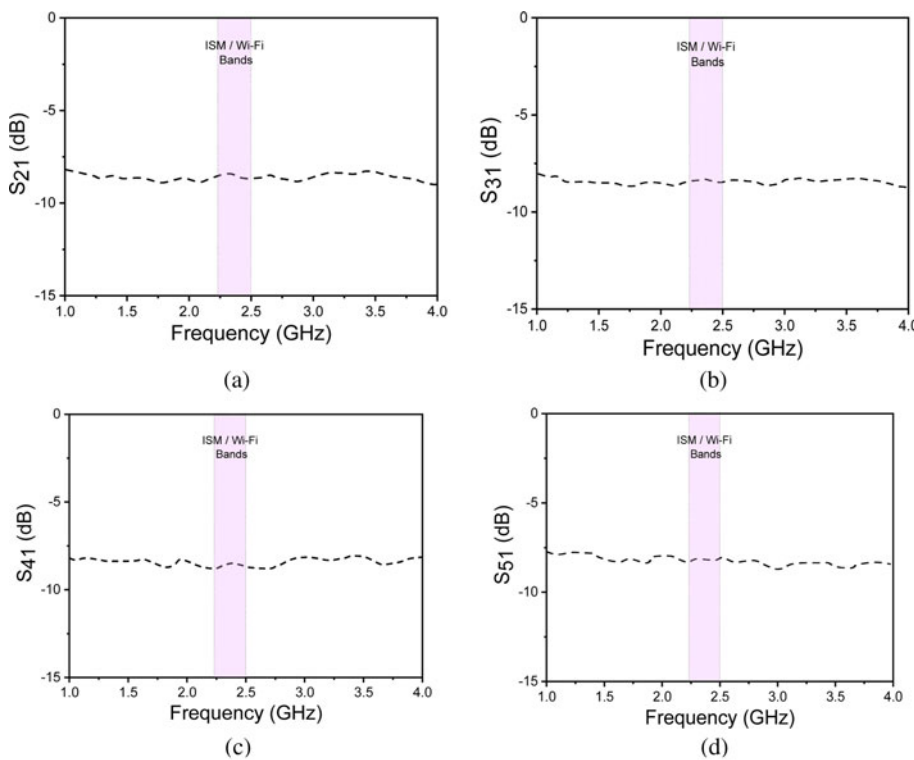


Fig. 9. Insertion loss of WPD with phase shifter IC 2484: (a) S_{21} , (b) S_{31} , (c) S_{41} , and (d) S_{51} .

with minimum side lobe of magnitude of -10.6 dB. In the H -plane, dipole patterns (figure of eight shape) are observed with main lobe magnitude of around 1 dB indicating an omnidirectional radiation with dominant null radiations occurring at an angle of 90° .

Figure 15 illustrates that the proposed dipole antenna radiates with an efficiency of $>78\%$ with gain closer to 5 dBi throughout the operating band (2.08–3.11 GHz). The gain and efficiency are calculated using the formula mentioned in [20]. It can also be visualized that there is minimum deviation between the simulated and measured results which may be due to fabrication tolerances.

Therefore, from the analysis and measurement of scattering and radiation performances, it is confirmed that the

proposed antenna is a good candidate for ISM/Wi-Fi applications and it can be easily integrated with the programmable phase shifter.

Proposed system design using PSoC

A proposed system is implemented using a combination of both custom hardware and PSoC processor to reconfigure analog and digital blocks in a real-time environment that permits the design to perform more than one function or adopt to perform better. The PSoC is used as a data acquisition and as beamforming controlling tool for higher sampling/conversion rate, to detect smaller change that can easily represent.

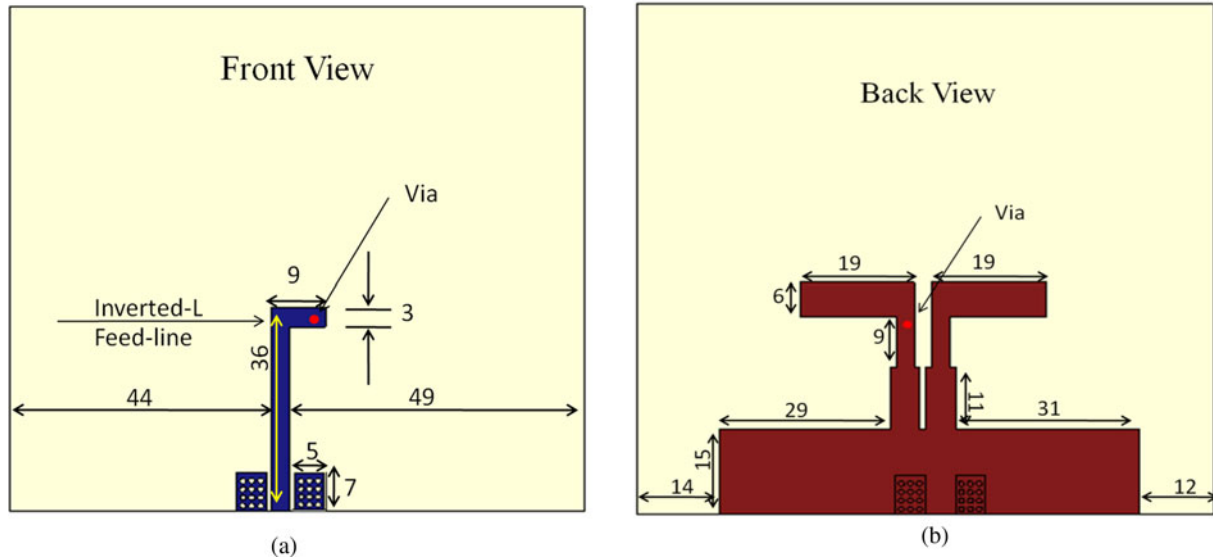


Fig. 10. Antenna geometry: (a) top view and (b) back view.

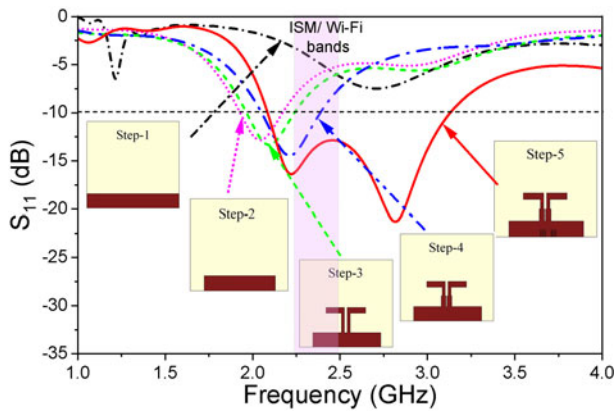


Fig. 11. Antenna ground plane evolution.

The 1×4 antenna array is constructed with a feed network that includes an RF source and a 1:4 power divider with the voltage controlled analog phase shifter IC. The array system was implemented for 2.45 GHz, four-element linear antenna array. The RF signal of 2.45 GHz is given as an input to the power divider. The power divider provides the same signal to the phase shifters. The block diagram of the proposed system for implementation and analysis using PSoC is shown in Fig. 1. Progressive phase shifts are controlled by PSoC for electronic beamforming.

As per the direction of arrival estimation, PSoC read and determine rotary encoder position and direction which provides the required biasing voltage for phase shifters and set progressive phase shifts for phased-array antenna elements. A beamforming system is developed using PSoC, which provides the optimal balance between performance and development time.

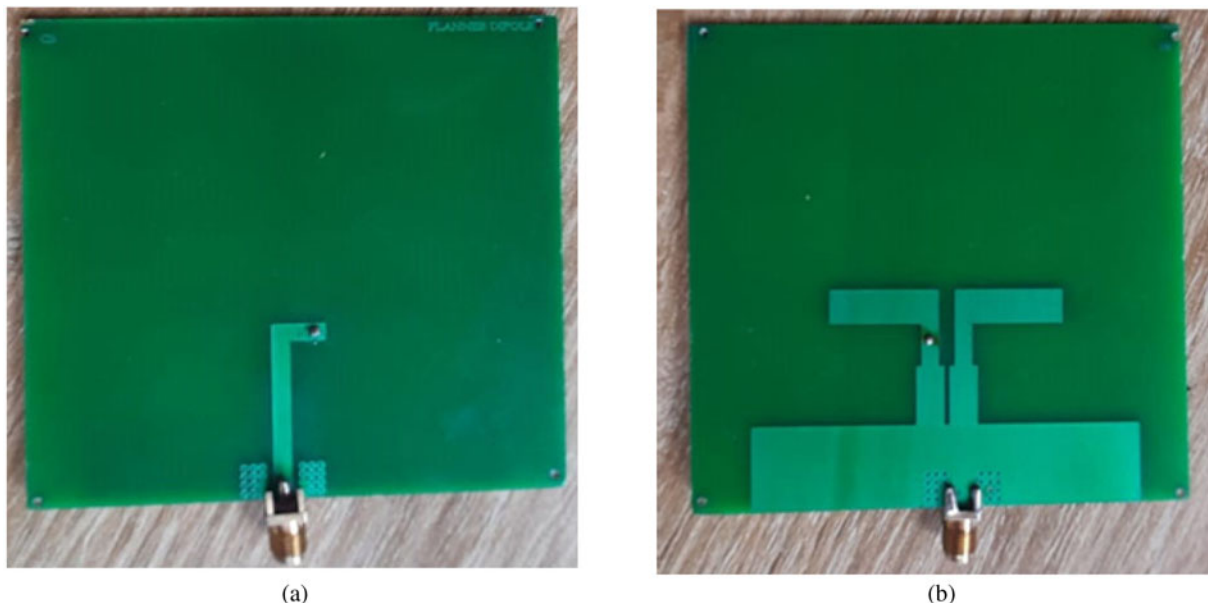


Fig. 12. Fabricated antenna geometry: (a) top view and (b) back view.

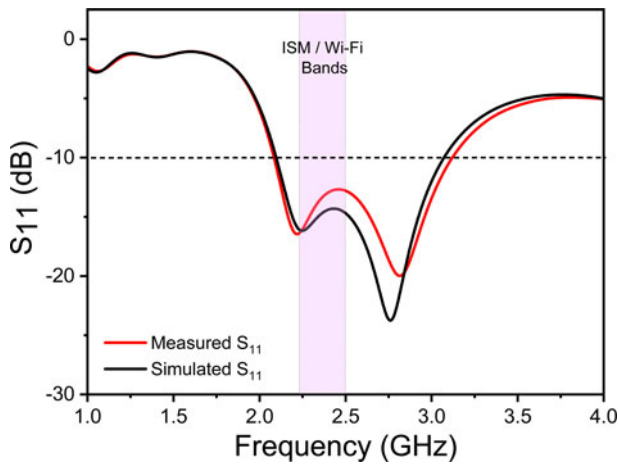


Fig. 13. Reflection coefficient S_{11} (dB) versus frequency (GHz) curves.

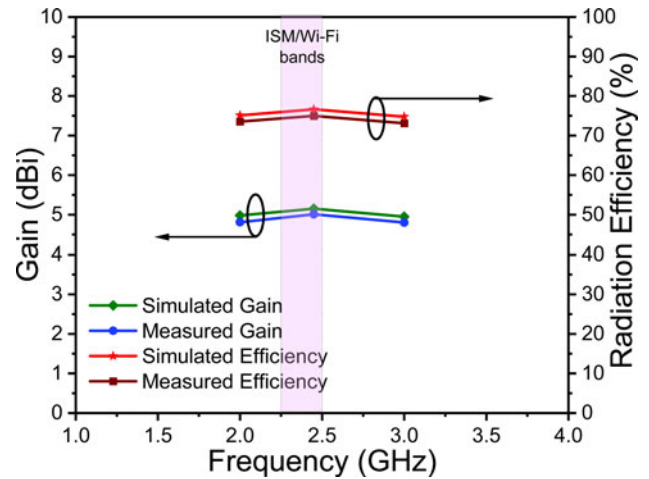
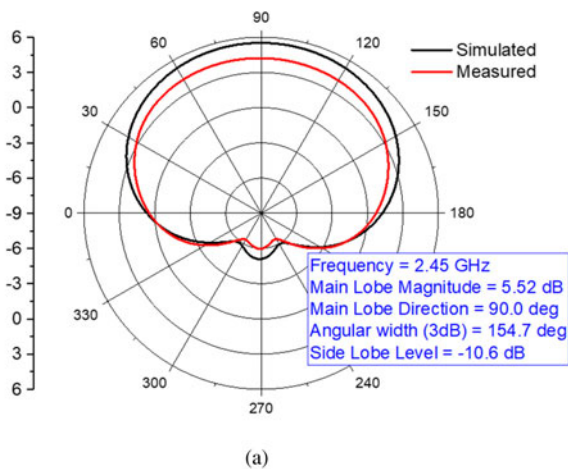
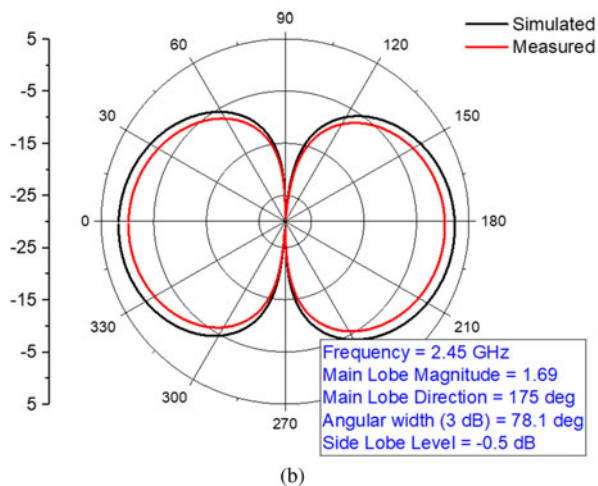


Fig. 15. Gain and efficiency.



(a)



(b)

Fig. 14. Radiation patterns at 2.45 GHz: (a) E-plane and (b) H-plane.

Block diagram of PSoC creator IDE

Programming a PSoC is a combination of drag and drop components and wiring and programming in C code. Following component icons such as IDAC, Character LCD, GPIO, and MUX are used for an embedding PSoC Creator IDE for the proposed

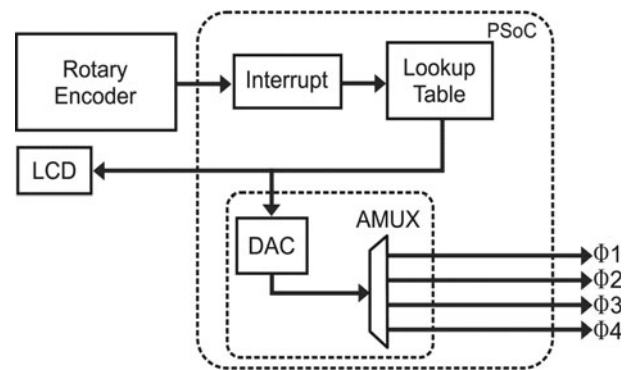


Fig. 16. Block diagram to set control voltage to generate progressive phase shift using PSoC 4 Creator IDE.

system. Figure 16 shows the block diagram that provides a detailed execution of the program to set the control voltage for the phase shifter IC 2484 through the PSoC and generate progressive phase shifts for the 1×4 phased array.

Flowchart of PSoC

The flowchart in Fig. 17 shows the step-by-step execution of PSoC, integrated development environment (IDE). The flowchart which gives step by step execution to write the program for PSoC creator IDE is shown in Fig. 16.

Progressive phase shifts are controlled by PSoC for electronic beamforming. Both numerical and empirical investigations are undertaken to measure performance. In the real-time environment when it comes in linking the RF components with software is always been one of the biggest challenges as it requires an understanding of RF-specific concepts which demand more attention for proper tuning than conventional circuit design, facing difficulties in adapting new environment, cope up to meet required new functionalities, ensuring smooth integration, consumes low power, testing and operating speed. This study is one of the first to demonstrate beamforming using PSoC which operates at 2.45 GHz frequency. In this proposed system, we successfully embed both RF component and PSoC controller together in such way that control voltages set for each phase shifter will

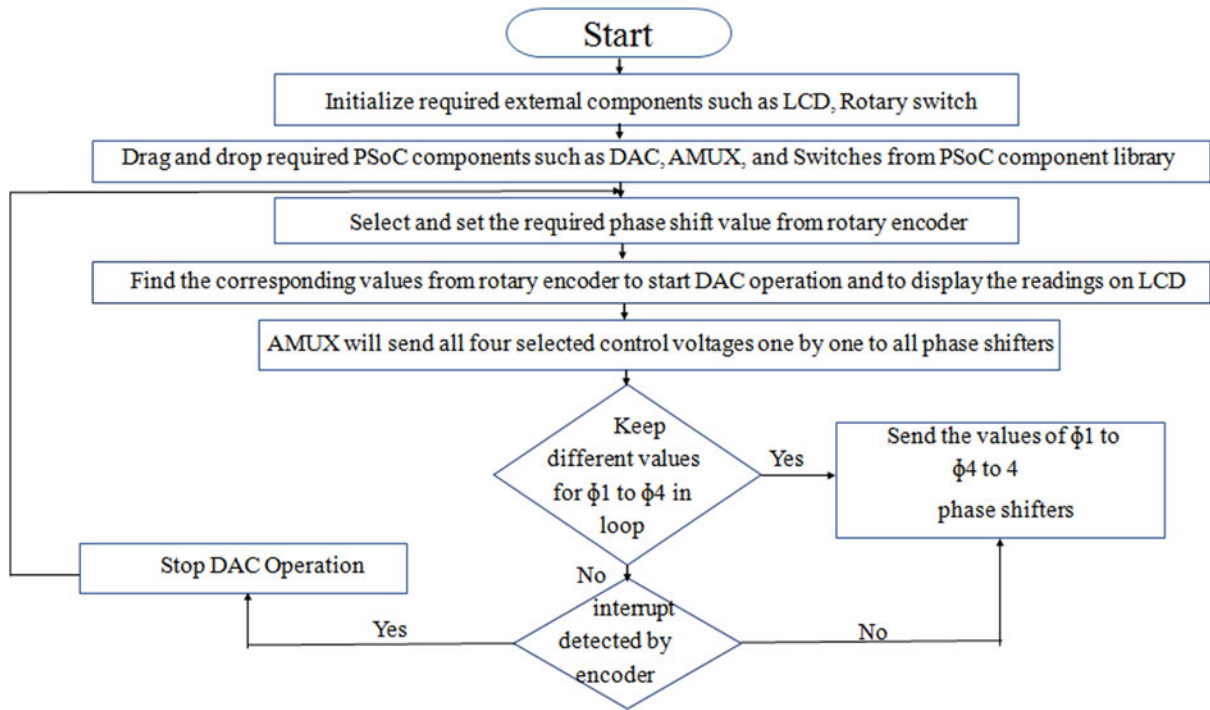


Fig. 17. Flowchart for PSoC Creator IDE.

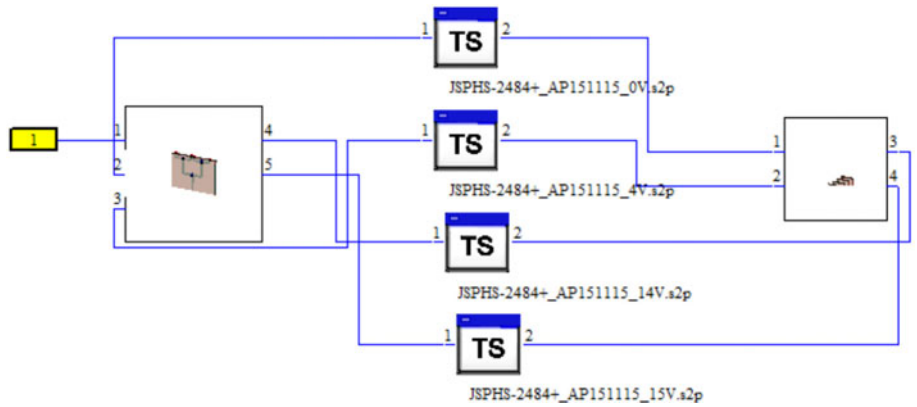


Fig. 18. Simulated schematic view of phased-array antenna with s_2p file of IC 2484.

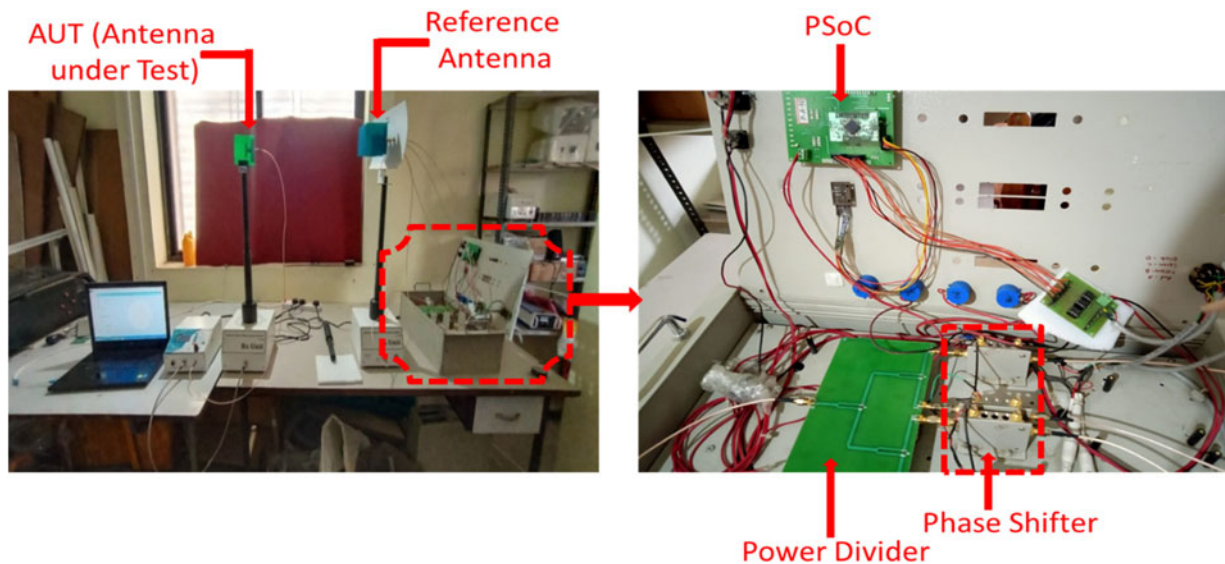


Fig. 19. Experimental set up for the validation of the programmable phase shifter.

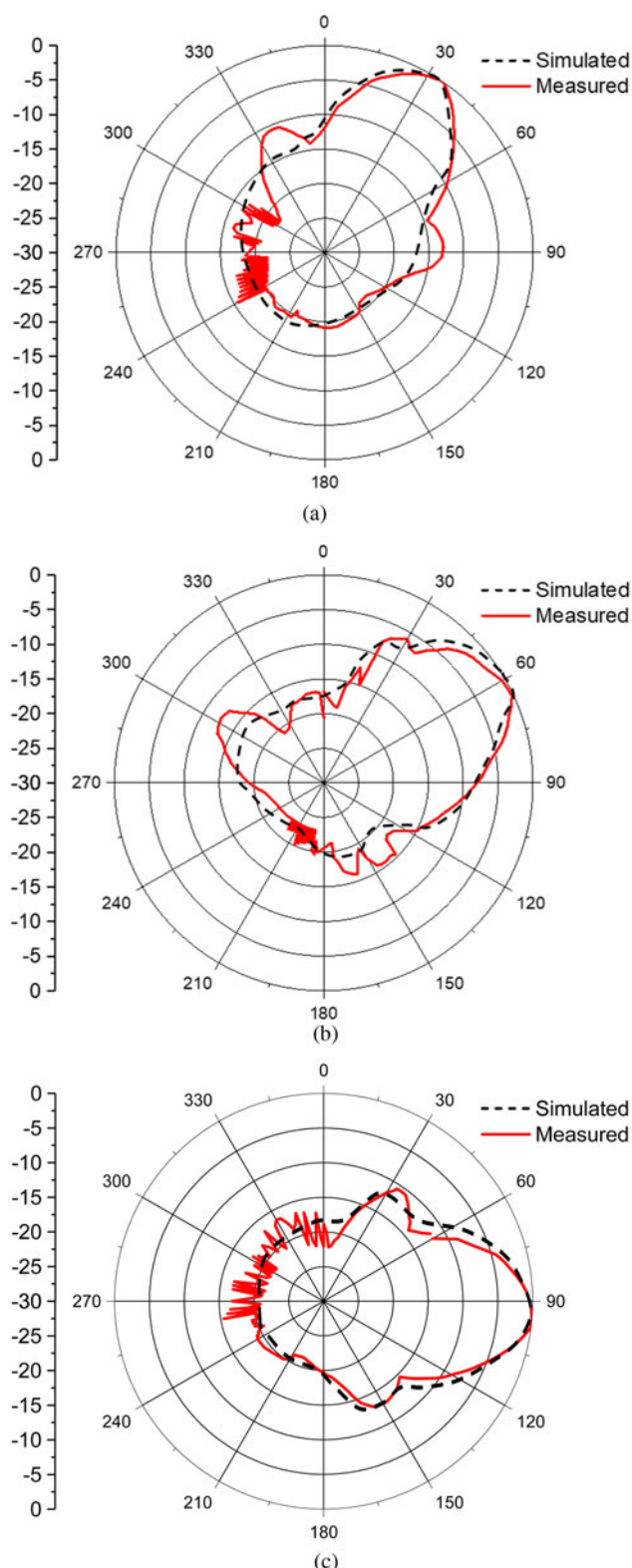


Fig. 20. Simulated and measured radiation beam patterns at (a) 30°, (b) 60°, and (c) 90°.

generate the beam pattern that is directive and steered successfully with great cross polarization level (XPD level). It is noted that in the proposed system, speed of excitation of phases are not affected the beam performance and the progressive phase shift obtained within $\pm 5\%$ accuracy which is used to steer the beam in the

desired direction. Results show that the proposed method provides a good estimation of relative system performance, which can be useful as a criterion choice for selecting the PSoC-embedded platform. After building the program in the PSoC processor, it works freely at the site of work for controlling or for detecting some input.

Simulated and measured phased-array antenna

Furthermore, the entire system is designed and simulated using CST software to observe the performance when used in a 1×4 antenna array. Depending upon the control voltage set by the PSoC, s_p^2 files of IC 2484, the progressive phase shifts are generated which is provided to the 1×4 phased array. A schematic view of the simulated phased-array antenna using a s_p^2 file of IC 2484 is displayed in Fig. 18.

To validate the progressive beam patterns, the phased-array antenna system is assembled as shown in Fig. 19 along with subsystem components such as WPD, phase shifter, a controlled circuit using PSoC, and four-element antenna arrays along with an Antenna Measurement System CISPER 1-1-1.

The radiation patterns for different scan angles of 30°, 60°, and 90° are plotted in Figs 20(a)–20(c) for experimental and simulated phased-array antennas. From Figs 20(a)–20(c), it is visualized that the simulated and measured beam patterns match accurately which clearly shows the correctness of control circuit designed using PSoC.

Moreover, it is also observed that the gain degradation in the measured results may be due to losses in the feed network, cables, and connectors used in the experimental setup. The average simulated and measured gain is 13.48 and 13.03 dBi, respectively in the operating band. It is observed that the experimental gain is less than the simulated gain by 0.45 dBi. The level of the side lobe discrepancies may be due to the infinite ground plane assumed in the simulation and the finite ground plane used in the fabricated array. However, SLL is maintained below -13 dB in both the cases. This shows that the accuracy of calibration of progressive phase angles is within limits.

Performance comparison of proposed design

Table 1 shows the comparison of the proposed design with the existing state-of-the-art in terms of power distribution, operating frequency, number of output ports, and design process of phase shifters, insertion loss, and gain of complete system.

From Table 1, it can be observed that the designed four-output power divider is uniform in nature and operates at the 2.45 GHz band. The designed phase shifter is simple and it uses an innovative PSoC technique to generate beam patterns at the desired phase angles. The complete design has low insertion loss and VSWR. The system has a high gain >13 dB in the operating band.

Conclusion

In this study, a phased-array antenna realized using a dipole antenna as the basic element combined with the power divider and PSoC-based phase shifter is proposed. Dipole antenna covers IBW of 39.69% with directional radiation patterns. Measured S_{21} , S_{31} , S_{41} , and S_{51} are -6.25 , -6.31 , -6.28 , and -6.31 dB, respectively, for power the divider which are very low and shows good agreement with the simulated values. A high-performance analog phase shifter using IC 2484 is analyzed, simulated, calibrated, and

Table 1. Performance comparison of various types of reported phase shifters

Ref.	Power distribution	Operating frequency (GHz)	No. of output ports	Design process of phase shifters	VSWR	Insertion loss (dB)	Gain (dBi)
[4]	Non-uniform	28	6	Not used	–	–	16.56
[5]	Uniform	1.5	2	TLs	–	–6	–
[6]	Uniform	2.4/3.6	2	Loaded and switched line using PIN diodes	1.08	–	12.6
[20]	Uniform	5	4	Varactor diodes	–	–	11
[21]	Uniform	5.2	4	Reconfigurable defected microstrip structure	–	2	10
[22]	Uniform	12	16	CRLH-TL	2	–	8.1
This study	Uniform	2.45	4	PSoC	1.58	–1.8	13.48

tested at an ISM band. The phase shifter has low variation in the insertion loss which leads to successful transmission in the linear array antenna. After deducting the insertion loss due to the power divider, the net insertion losses that occur due to the phase shifter at ports 2, 3, 4, and 5 are -1.73 , -1.88 , -1.78 , and -1.84 dB, respectively. The average value of the insertion loss is -1.80 dB which is well within the specified value of 5.6 dB. The radiation patterns for different scan angles of 30, 60, and 90° are plotted for phased-array antenna where simulated and measured beam patterns match accurately which clearly shows the correctness of the control circuit designed using PSoC.

References

- Bhattacharyya AK (2006) *Phased Array Antennas: Floquet Analysis, Synthesis, BFNs and Active Array Systems*, 1st Edn. Newark, NJ, USA: Wiley-Interscience.
- Bhartia P, Bahl I, Garg R and Ittipiboon A (2000) *Microstrip Antenna Design Handbook*. Norwood, MA, USA: Artech House Publishers.
- Balanis CA (2015) *Antenna Theory: Analysis and Design*. Hoboken, NJ, USA: John Wiley & Sons.
- Uddin MN and Choi S (2020) Non-uniformly powered and spaced corporate feeding power divider for high-gain beam with low SLL in millimeter-wave antenna array. *Sensors* **20**, 4753.
- Wang EC, Fu XY and Tian Q (2012) Broadband power divider with phase shifter. 2012 2nd International Conference on Consumer Electronics, Communications and Networks (CECNet), pp. 1700–1702.
- Kodgirwar VP, Deosarkar SB and Joshi KR (2020) Design of beam steering-switching array for 5G S-band adaptive antenna applications – part-I and part-II. *IETE Journal of Research*, 1–13.
- Varadan VK, Jose KA, Varadan VV, Hughes R and Kelly JF (1995) A novel microwave planar phase shifter. *Microwave Journal* **38**, 244–249.
- Chang C, Guo L, Tantawi SG, Liu Y, Li J, Chen C and Huang W (2015) A new compact high-power microwave phase shifter. *IEEE Transactions on Microwave Theory and Techniques* **63**, 1875–1882.
- Padilla JL, Padilla P, Valenzuela-Valdés JF and Fernández JM (2014) High-frequency radiating element and modified 3 dB/90° electronic shifting circuit with circular polarization for broadband reflectarray device cells. *Electronics Letters* **50**, 1042–1043.
- Jacobs H and Chrepta MM (1974) Electronic phase shifter for millimeter-wave semiconductor dielectric integrated circuits. *IEEE Transactions on Microwave Theory and Techniques* **22**, 411–417.
- Abdollahy H, Farahbakhsh A and Ostovarzadeh MH (2021) Mechanical reconfigurable phase shifter based on gap waveguide technology. *AEU-International Journal of Electronics and Communications* **132**, 153655.
- Hum SV and Perruisseau-Carrier J (2014) Reconfigurable reflect arrays and array lenses for dynamic antenna beam control: a review. *IEEE Transactions on Antennas and Propagation* **62**, 183–198.
- Zhao Z, Wang X, Choi K, Lugo C and Hunt AT (2007) Ferroelectric phase shifters at 20 and 30 GHz. *IEEE Transactions on Microwave Theory and Techniques* **55**, 430–437.
- Kingsley N, Ponchak GE and Papapolymerou J (2008) Reconfigurable RF MEMS phased array antenna integrated within a liquid crystal polymer (LCP) system-on-package. *IEEE Transactions on Antennas and Propagation* **56**, 108–118.
- Basu A and Koul SK (2009) Theory and design of solid-state microwave phase shifters. *IETE Journal of Education* **50**, 9–18.
- Yusuf Y and Gong X (2008) A low-cost patch antenna phased array with analog beam steering using mutual coupling and reactive loading. *IEEE Antennas and Wireless Propagation Letters* **7**, 81–84.
- Zhang H-Y, Zhang F-S, Zhang F, Sun F-K and Xie G-J (2017) High-power array antenna based on phase-adjustable array element for wireless power transmission. *IEEE Antennas and Wireless Propagation Letters* **16**, 2249–2253.
- Yang G, Li J, Wei D and Xu R (2017) Study on wide-angle scanning linear phased array antenna. *IEEE Transactions on Antennas and Propagation* **66**, 450–455.
- Loghmannia P, Kamyab M, Nikkhah MR and Rezaiesarlak R (2012) Miniaturized low-cost phased-array antenna using SIW slot elements. *IEEE Antennas and Wireless Propagation Letters* **11**, 1434–1437.
- Ji Y, Ge L, Wang J, Chen Q, Wu W and Li Y (2019) Reconfigurable phased-array antenna using continuously tunable substrate integrated waveguide phase shifter. *IEEE Transactions on Antennas and Propagation* **67**, 6894–6908.
- Ding C, Jay Guo Y, Qin P-Y and Yang Y (2015) A compact microstrip phase shifter employing reconfigurable defected microstrip structure (RDMS) for phased array antennas. *IEEE Transactions on Antennas and Propagation* **63**, 1985–1996.
- Nikfalazar M, Sazegar M, Mehmood A, Wiens A, Friederich A, Maune H, Binder JR and Jakoby R (2016) Two-dimensional beam-steering phased-array antenna with compact tunable phase shifter based on BST thick films. *IEEE Antennas and Wireless Propagation Letters* **16**, 585–588.
- Yang H, Cao X, Gao J, Yang H and Li T (2020) A wide-beam antenna for wide-angle scanning linear phased arrays. *IEEE Antennas and Wireless Propagation Letters* **19**, 2122–2126.
- Tsai J-H, Liu C-K and Lin J-Y (2014) A 12 GHz 6-bit switch-type phase shifter MMIC. *Proceedings 44th European Microwave Conference*, pp. 1916–1919.
- Cetindogan B, Ozeren E, Ustundag B, Kaynak M and Gurbuz Y (2016) A 6-bit vector-sum phase shifter with a decoder-based control circuit for X-band phased-arrays. *IEEE Microwave and Wireless Components Letters* **26**, 64–66.
- Hosseinnezhad M, Nourinia J and Ghobadi C (2017) Back radiation reduction of a printed Yagi antenna backed by a metalized reflector for C-band applications at 3.7–4.2 GHz. In *2017 IEEE 4th International Conference on Knowledge-Based Engineering and Innovation (KBEL)*, pp. 0828–0830.

27. **Kulkarni J, Kulkarni N and Desai A** (2020) Development of H-shaped monopole antenna for IEEE 802.11a and HIPERLAN 2 applications in the laptop computer. *The International Journal of RF and Microwave Computer Aided Engineering* **30**, 1–14.



Aparna Balaji Barbadekar has been working as assistant professor in the Department of Electronics and Telecommunication Engineering at Vishwakarma Institute of Information Technology, Pune, till date. She has received good and steady support from her parent institute and her guide.



Dr. Pradeep Mitharam Patil who is presently working as principal, SND College of Engineering and Research Center, Yeola District, Nashik, Maharashtra, India. He is member of various professional bodies such as IE, ISTE, IEEE, and Fellow of IETE. He has been recognized as a PhD guide by various Indian universities such as the University of Pune, Shivaji University, Kolhapur, and North Maharashtra University, Jalgaon. His research areas include pattern recognition, neural networks, fuzzy neural networks, and power electronics.